PERGAMON

Deep-Sea Research I 46 (1999) 1733–1753

DEEP-SEA RESEARCH
PART I

# Observations on the Rim Current structure, CIW formation and transport in the western Black Sea

Temel Oguz*, Sukru Besiktepe

*Middle East Technical University, Institute of Marine Sciences, P.O. Box. 28, Erdemli, 33731, Icel, Turkey*

Received 5 March 1998; received in revised form 17 July 1998; accepted 29 January 1999

**Abstract**

CTD and ADCP measurements together with a sequence of satellite images indicate pronounced current meandering and eddy activity in the western Black Sea during April 1993. The Rim Current is identified as a well-defined meandering jet stream confined over the steepest topographic slope and associated cyclonic–anticyclonic eddy pairs located on both its sides. It has a form of highly energetic and unstable flow system, which, as it propagates cyclonically along the periphery of the basin, is modified in character. It possesses a two-layer vertical structure with uniform upper layer speed in excess of 50 cm/s (maximum value $\sim$ 100 cm/s), followed by a relatively sharp change across the pycnocline (between 100 and 200 m) and the uniform sub-pycnocline currents of 20 cm/s (maximum value $\sim$ 40 cm/s) observed up to the depth of $\sim$ 350 dbar, being the approximate limit of ADCP measurements. The cross-stream velocity structure exhibits a narrow core region ($\sim$ 30 km), flanked by a narrow zone of anticyclonic shear on its coastal side and a broader region of cyclonic shear on its offshore side. The northwestern shelf circulation is generally decoupled from the influence of the basinwide circulation and is characterized by much weaker currents, less than 10 cm/s. The southward coastal flow associated with the Danube and Dinepr Rivers is weak during the measurement period and is restricted to a very narrow coastal zone.

The data suggest the presence of temperature-induced overturning prior to the measurements, and subsequent formation of the Cold Intermediate Water mass (CIW) within the Northwestern Shelf (NWS) and interior of the western basin. The newly formed shelf CIW is transported in part along the shelf by the coastal current system, and in part it flows downslope across the shelf and intrudes into the Rim Current convergence zone. A major part of the cold water mass, however, seems to be trapped within the northwestern shelf. The CIW mass,

* Corresponding author. Tel.: 90-324-521-2406; fax: 90-324-521-2327.
*E-mail address:* oguz@ims.metu.edu.tr (T. Oguz)


PII: S0967-0637(99)00028-X

injected into the Rim Current zone from the shelf and the interior region, is then circulated around the basin. 

## 1. Introduction

The western Black Sea (Fig. 1), covering the region to the west of 35°E longitude, possesses a SW–NE oriented rectangular deep basin, about 2000 m deep, and a fairly wide shelf (equivalent to about 15% of the surface area of the sea) on its northwestern section (henceforth, the shelf is referred to as NWS). The NWS is almost triangular, narrowing gradually towards the south along the Romanian, Bulgarian coast. The continental slope, defined as the region between the 100 and 2000 m topography contours, attains the same width as that of the shelf and therefore is much wider to the southwest of the Crimean peninsula. This relatively smooth transition zone between the northwestern shelf and the deep basin is also called the "Danube Fan". Along the Turkish coast, the shelf terminates abruptly near the Sakarya Canyon region (31°E), east of which, there is a very narrow shelf and a steep continental slope.

The Rim Current is a band of permanent, strong current system encircling the basin cyclonically over the continental slope zone. Hydrographic studies (e.g. Oguz et al., 1993,1994,1998) and satellite-derived thermal patterns and CZCS pigment distributions

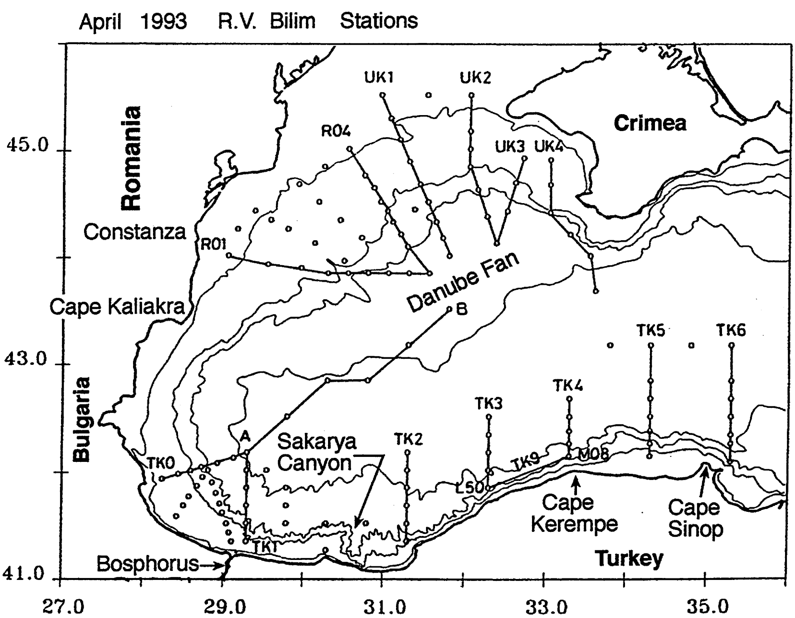


Fig. 1. The station network and bathymetry of the Black Sea with the sections referred to in the text. The bathymetry includes only 50, 200, 1000 and 2000 m contours.

(e.g. Oguz et al., 1992; Sur et al., 1994,1996; Sur and Ilyin, 1997) suggest extreme mesoscale variability of the circulation. This includes different types of structural organizations of the interior cyclonic gyre as well as meanders, eddies and filaments associated with the Rim Current. The Rim Current is also identified by a distinct thermohaline structure between fresher (less dense) coastal/shelf water and saltier (denser) interior water. The salinity signature of this frontal zone becomes more dominant during the summer at the times of increased river runoff, whereas the temperature signal governs the thermohaline structure during the winter corresponding to the period of cold water mass formation.

The Rim Current structure is accompanied by a series of localized quasi-stable/recurrent coastal anticyclonic mesoscale eddies as well as transient waves with an embedded train of mesoscale eddies propagating cyclonically around the basin (cf. Sur et al., 1994; Sur et al., 1996; Ovchinnikov et al., 1994). Analyzing all the available published hydrographic data up to 1990, Oguz et al. (1993) proposed nine such quasi-stable/recurrent coastal eddies (cf. Fig. 12 in Oguz et al., 1993). Their origin was related to the control of the Rim Current by local geometric and topographic features and/or meteorological forcing (Oguz et al., 1992). However, due to the limited clear sky satellite scenes available, it is not possible to provide an independent support from the satellite data and, therefore, to distinguish definitely quasi-permanent eddies from a chain of different eddies passing through one after the other from the same location.

The southwestern Turkish coast to the east of the Bosphorus up to the Cape Sinop and the Caucasian coast along the northern periphery of the eastern basin are two particular regions where transient meandering features of the Rim Current were mostly studied. On the contrary, flow characteristics over the topographic slope zone extending from the west of the Crimean peninsula to the Turkish coast near the Bosphorus (see Fig. 1) received much less attention. Mesoscale variability of the Rim Current of this relatively unexplored sector of the Black Sea will be one emphasis of this paper.

Sur et al. (1994) provided a sequence of CZCS images for the period 9 June–26 June 1980 showing eastward propagating waves along the Turkish coast between 30°E and 34°E longitudes with an appreciably fast propagation speed of 10–15 km/d and a typical wavelength of about 100 km superimposed on the Rim Current. They suggested that the flow, which is apparently in a state of geostrophic balance upstream along the western coast, is perturbed by the discontinuity in shelf topography and sudden depth changes at Sakarya Canyon, modified later by changes in the coastline orientation, and evolves eventually into the form of strong meanders, unstable eddies and filaments on time scales of a few days as a result of baroclinic instability. Satellite images for the summer 1992 revealed similar propagating meanders and eddying motion along the southwestern coast of the Black Sea (Sur and Ilyin, 1997). The wavelengths of the meanders were estimated to lie between 78 and 88 km, whereas the translation speed varied in the range 2.0–4.5 km/d between May and July. Slow translation rates of mesoscale features were also pointed out for the same region earlier by Oguz et al. (1992), Sur et al. (1994) and Sur and Ilyin (1997). The long-term (5.5 y) continuous hourly current measurements from a buoy station located on the north Caucasian shelf indicated, on the average, passage of 32 waves per year

(Ovchinnikov et al., 1994). The wavelength of most unstable waves was estimated to be about 80–90 km. The winter-to-summer changes on the stability characteristics of the Rim Current structure, however, deserves further observational and modeling studies.

During April 1993, as part of an international multi-disciplinary study, we carried out CTD and acoustic doppler current profiler (ADCP) measurements in the western Black Sea. This survey provided, for the first time, a unique set of direct, "absolute" current measurements involving both baroclinic and barotropic components. (In the past, our understanding of the vertical current structure was, limited to the geostrophic calculations.) In this paper, we present findings from this survey. Following the description of the data collection and processing methodology in Section 2, we provide a three dimensional, quasi-synoptic view of the regional flow field representative of the late winter-early spring season (Section 3). One of our two primary emphasis here is to document the ADCP-based Rim Current vertical structure at several cross-sections along the NWS and the Anatolian coast, and to compare them with those computed from the hydrographic data only (Section 3.1). The other is to describe the mesoscale variability of the circulation using a combination of the CTD, ADCP-based analysis and available cloud-free satellite imagery for the April 1993 period (Sections 3.2 and 3.3). Furthermore, because it is one of the rare data sets representing the late winter conditions of the Black Sea (most previous surveys were during the summer months), our next objective is to study late winter-early spring evolution of the Cold Intermediate Water mass (CIW) with particular emphasis on its formation and subsequent transport characteristics (Section 4). The role of mesoscale eddies located along the continental slope of the western basin on the shelf-slope exchanges of the CIW is also explored in this section. A summary and conclusions are provided in Section 5.

## 2. Data

The Turkish ship R.V. Bilim acquired CTD data at a series of cross-shelf sections and monitored currents with ADCP measurements in the Turkish waters as well as within the Ukranian and Romanian Exclusive Economic Zones (EEZ) of the NWS during 2–15 April 1993. The measurements were performed on a series of sections covering a major part of the northwestern continental shelf and slope with some limited extension into the basin's interior (Fig. 1). Along the southern coast, sampling was taken across several meridional sections extending approximately 100 km offshore. The station spacing along these sections was variable, changing from about 2 miles to 10 miles depending on water mass characteristics and steepness of the topographic slope. However, spacing between these sections, was generally coarser than the resolution necessary to capture the mesoscale features, especially along the Turkish coast. The sampling period was calm, characterized by light easterly winds, and the low-pass filtered winds measured on board were less than 5 m/s.

The hydrographic observations were made with a SeaBird SBE-9 CTD system lowered at an approximate rate of 30–45 m/min to a maximum depth of 500 m or to a few meters above the bottom over the continental shelf and upper slope. The measurements that were carried out only within the upper 500 m of the water column is justified for this survey, since the main interest was to study the physical and biogeochemical properties of the upper layer. Because of the well-established two-layer density structure of the Black Sea, a strong permanent pycnocline located at 100–150 m depths separates two distinctly different water mass structures. Inside the lower layer, the water mass properties change only little below 300 m depth and hardly at all below 500 m depth. This choice improves considerably the synopticity of the survey.

The CTD data were processed to yield potential temperature, salinity and density over 1 dbar bins. Vertical profiles of E–W and N–S current components were obtained continuously along the ship track using a vessel mounted 200 kHz ADCP manufactured by RD Instruments. In deeper parts of the analysis region, currents were measured for a depth range varying generally between 150 and 250 m, and even for greater depths up to 400 m at some selected stations. The measurements were made at a rate of 1 ping per second. We used an ensemble averaging period of 10 min, and pulse and vertical bin lengths of 4 m in the RD data collection software called "Collect". The data were rejected when the percent-good criterion fell below 80%. Over the shelf, where bottom tracking of the beam was possible, the ensemble averaging period and bin length were reduced to 5 min and 2 m, respectively. The current profiles are generally reliable from $\sim$8 m below the surface to within 15–25 m of the bottom, depending on the water depth. Heading information obtained from the ship's gyrocompass was used to convert the velocities measured relative to the ship to the earth referenced coordinate. Ship speed, which was continually updated by the global positioning system (GPS) fixes, provided necessary correction for the reference layer velocity. The absolute velocity is then computed by subtracting the reference layer velocity from the velocity measured relative to the reference layer. The reliability of this procedure was checked by applying the same measurement technique in shallow regions, where bottom tracking was in fact able to provide direct absolute velocity measurements. The error between these two types of absolute current velocity measurements was found to be not more than 5 cm/s. For more details on the ADCP processing, we refer to Firing et al. (1991).

In addition to the R.V. Bilim CTD and ADCP measurements at stations shown in Fig. 1, a quasi-simultaneous CTD survey was accomplished independently over the entire western basin up to 35°E longitude. The Ukranian ship R.V. Kolesnikov covered the northern part, and another Turkish ship, R.V.K. Piri Reis, performed the measurements in the southern part of the western region. A SeaBird SBE-9 CTD system was used on the R.V.K. Piri Reis. The R.V. Kolesnikov used a Vistok 7 CTD system, which has sensor characteristics comparable with those of the SeaBird SBE-9. All measurements were calibrated with respect to several deep intercalibration stations. The measurements were made over a 20 mile station network within the interior part of the basin. The station spacing along the meridional sections was reduced to 10 miles or less in coastal regions and over the steep slope zones. The spacing between the meridional sections was about half a degree (i.e. approximately 30 miles). The positions of most of the stations visited by these ships during April 1993 are superimposed on the 10 dbar dynamic height anomaly field given in Fig. 2.

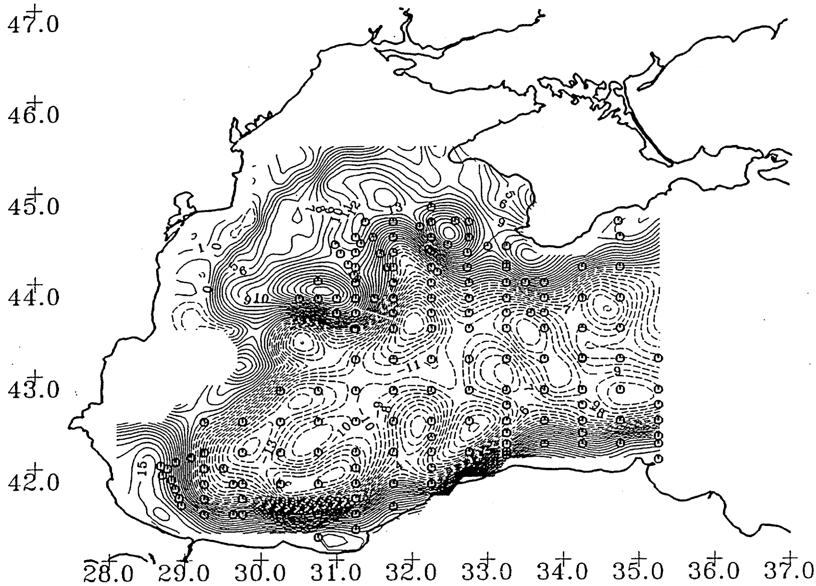


Fig. 2. 10 bar dynamic height (cm) anomaly field for the western Black Sea (after Gungor, 1994). The level of no motion is taken at 500 dbar level. Circles denote stations included in the dynamic height analysis.

## 3. Description of the regional flow field

The presence of a complex, eddy-dominated flow field and the strength of the Rim Current appear as the two significant features of the April 1993 circulation. In this section, first the Rim Current vertical structure is described, using ADCP measurements at selected cross-sections, and compared with the geostrophic currents. Next, the main horizontal circulation features are presented for the northwestern-western and the southern coastal zones of the western Black Sea.

### *3.1. Vertical structure of the Rim Current*

As inferred from the 10 dbar dynamic height field (Fig. 2), computed using a multivariate objective analysis of the ADCP and CTD data (Gungor, 1994; see McWilliams et al., 1986 for the general description of the method), the current in the northern part of the region is rather broad, spreading over the wide continental slope. It reaches an average speed of 50 cm/s inside the core of the jet within the entire upper layer (Fig. 3). Below the depth of the permanent pycnocline ($\sim$125 dbar), the currents decrease and have a magnitude of about 25 cm/s at 200 dbar. The current intensity changes significantly across the shelf break. Over the shelf, the currents are of the order of 10 cm/s in the upper levels and decrease slightly towards the bottom.

Along the Turkish coast, the flow field reveals a much stronger and tighter current system with considerable cross-stream structure. As shown by TK1 and TK5 (Figs. 4

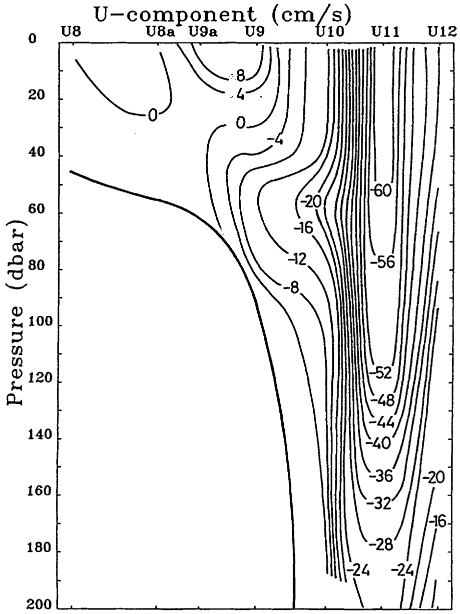


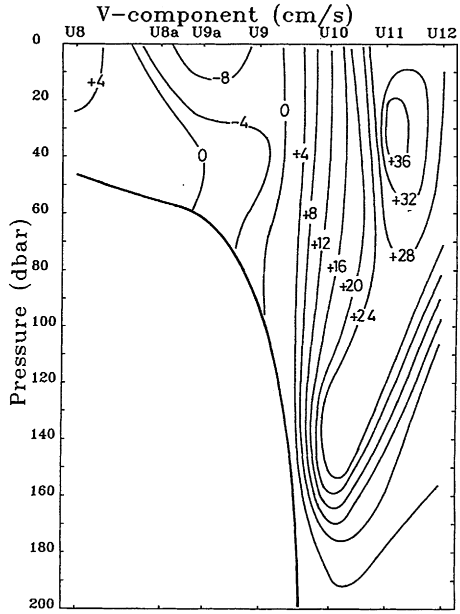


Fig. 3. Vertical sections of the U (eastward) and V (northward) components of the ADCP currents (cm/s) for section UK2.

and 5a), the jet is confined to the upper continental slope close to the shelf break and has a width of less than $\sim 30$ km. It has nearly uniform maximum speed of $\sim 70$ cm/s within the upper 100 m, therefore possessing no appreciable vertical shear above the permanent pycnocline. As shown previously in Fig. 3, a sharp decrease in the intensity of the flow across the pycnocline is followed by approximately uniform current structure below. In both sections, the lower layer current reaches about 20 cm/s within the core of the jet. The most intense currents of $\sim 100$ cm/s are measured here along section TK9 (Fig. 6). Below the pycnocline, the vertically uniform currents in the range 20–40 cm/s are measured upto $\sim 300$ dbar. We think that this current behavior is strongly reminescent of a purely inertial jet, tightened by potential vorticity conservation and accelerating under the constraint of the Bernoulli function conservation.

A comparision of the currents obtained directly by ADCP measurements with those computed indirectly from the hydrographic data using linear, geostrophic dynamics may be instructive and allows us to estimate how our classical geostrophic computations underestimate currents, especially at sub-pycnocline levels. In the present analysis, the geostrophic currents were calculated using the dynamic height field relative to 500 dbar, which was the lower limit of the CTD measurement. Because of the uniformity of the water mass properties below 300 m depth (both horizontally and vertically), this choice of the reference level does not introduce any serious error. This was verified before in the September 1990 survey, in which hydrographic casts were generally made all the way to the bottom (Oguz et al., 1993). The computations

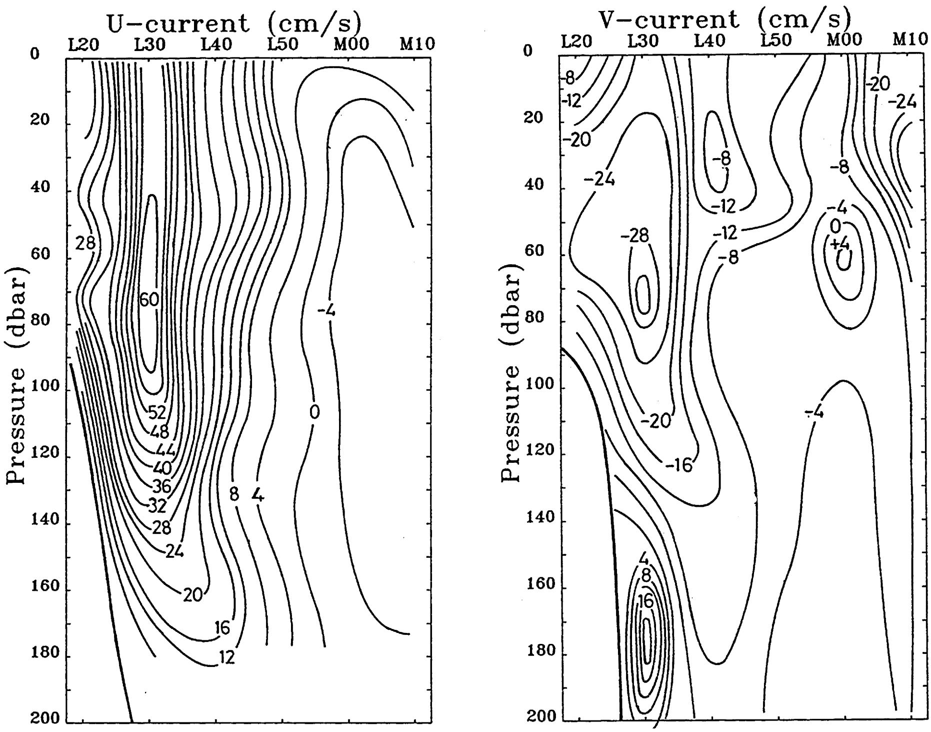


Fig. 4. Vertical sections of the U (eastward) and V (northward) components of the ADCP currents (cm/s) for section TK1.

indeed provided nearly two orders of magnitude difference between values of the surface and 500 dbar dynamic height fields computed relative to a 1500 dbar level of no motion. This is the main reason for the Black Sea circulation and thermohaline characteristics below 300 m depth to remain relatively unexplored.

The vertical current structures for section TK5 are presented in Figs. 5a and b. We note that this section lies almost perpendicular to the zonally oriented Turkish coast. It is chosen particularly because the currents are nearly unidirectional, flowing along the coast with negligible contribution from the other component. Thus, the two current structures may be compared without introducing any appreciable error. The most noticeable difference between Figs. 5a and b are observed within the jet core. The magnitudes of currents away from the jet are comparable with each other, as can be noted from the structures around station M50. The geostrophic currents, however, tend be become weaker towards the jet and differ considerably from the ADCP currents inside its core at the sub-pycnocline levels. This is due to considerable reduction in the vertical and horizontal gradients between the coastal and interior waters at depths below the permanent pycnocline, as can be noted from the temperature and salinity transects for this section (Fig. 12). Consequently, the geostrophic

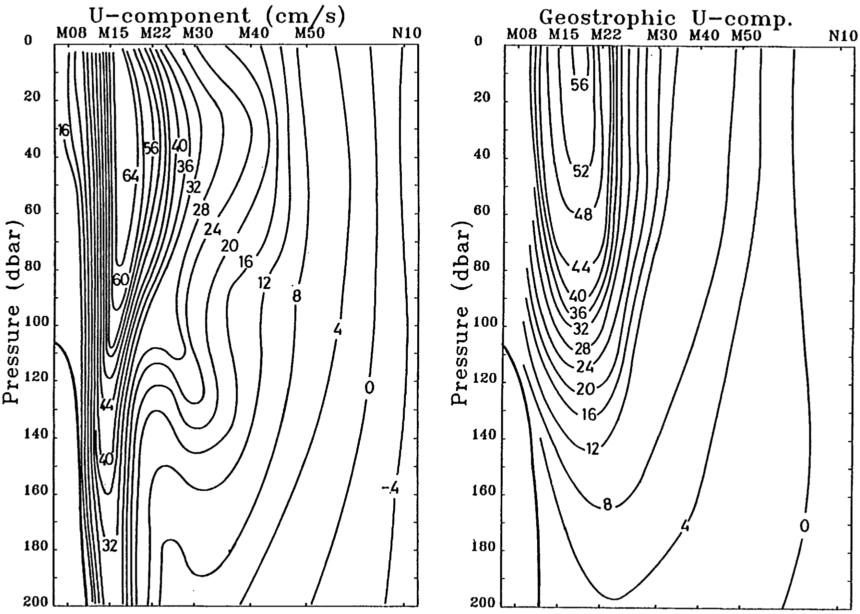


Fig. 5. Vertical sections of the U (eastward) components of the currents (cm/s) (a) measured by the ADCP, and (b) computed geostrophically from the density data for section TK5.

current decreases to about 15 cm/s at 150 m depth, contrary to more than 30 cm/s currents measured by the ADCP. Furthermore, because of its much higher sampling resolution, the ADCP data provide much sharper and well-defined horizontal jet structure.

The differences shown in Figs. 5a and b are typical of all the sections shown in Fig. 1, including the northwestern shelf/slope region, and therefore more examples are not given here. On the other hand, Ginsburg et al. (1998) provide two geostrophically computed current sections (referenced to 500 dbar) corresponding approximately with our sections UK1 and UK2 in Fig. 1. The measurements were performed during 16–17 April 1993, just a few days after the R.V. Bilim survey in the region. They also reveal geostrophic currents of the order of 10 cm/s (minimum 4 cm/s, maximum 15 cm/s across the jet core) at 150 m depth, and up to 5 cm/s at 300 m depth.

### 3.2. *Mesoscale features along the northwestern–western sector*

The 10 dbar circulation map for the April 1993 survey (Fig. 2) together with the 19 April 1993 AVHRR satellite picture (Fig. 7), which is the nearest available cloud free scene, indicate a series of meanders and associated cyclonic–anticyclonic eddy pairs in the region between the west coast of the Crimean peninsula on the north and the Turkish coast to the west of the Bosphorus on the south. The Rim Current flowing over the topographic slope south of Crimea deflects slightly towards the NWS near

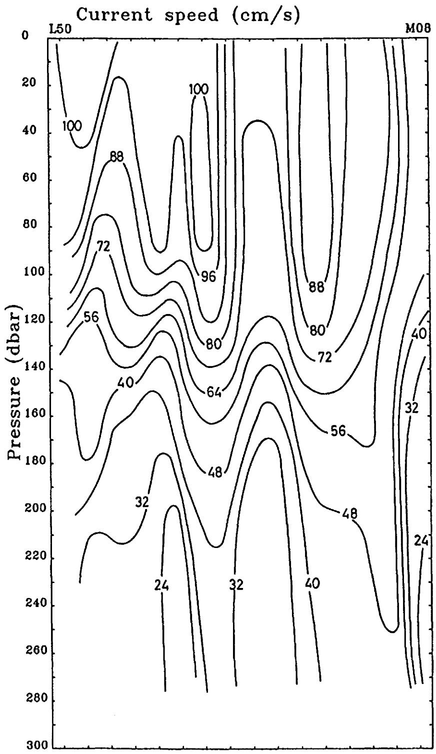


Fig. 6. Vertical section of the ADCP current speed (cm/s) along section TK9.

32°E, following the bottom topography. Near the shelf break, during its onshelf excursion, the flow is separated into two branches. One branch forms the anticyclonic eddy, designated in the satellite picture as A1. It is centered at 44.7°N, 32.5°E, in Fig. 2, whereas, in the satellite picture representing the conditions 7 d later than the measurements taken along this section, it is identified as a cold water spot centered at 44.5°N and 32.1°E with a diameter of 55 km. This implies translation of the eddy southwestward over the topographic slope region, approximately 50 km in 7 d, and intrusion of a new meander (called M0 in Fig. 7) into the NWS region from the upstream direction.

The other branch of the flow turns cyclonically in the offshore direction and forms the meander M1. This branch is then steered topographically further south–southwestward and undergoes a series of successive bifurcations, forming eventually a second anticyclonic eddy off Constantza, named A2 in the subsequent analysis. This is again shown as a cold water spot centered at 44.2°N and 30.5°E in Fig. 7. On the other hand, a small part of the flow penetrates northward in the shelf along the western Crimean coast. It appears to turn anticlockwise to the north of the eddy A1 and joins the cyclonic circulation on the Romanian shelf. Although it is not particularly clear in Fig. 2 due to the measurement limitations in the near-coastal waters, the cyclonic eddy

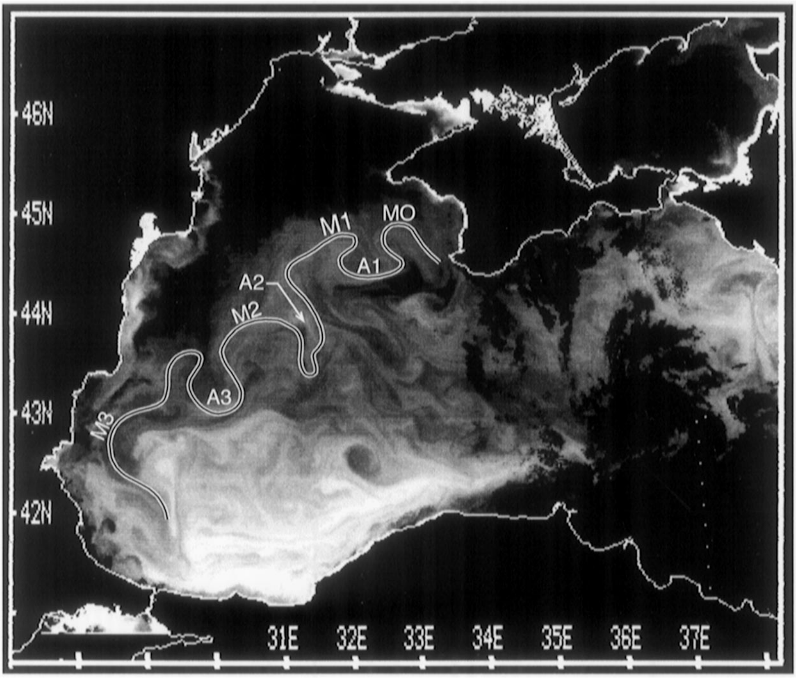


Fig. 7. NOAA 14 AVHRR imagery for 19 April 1993 showing the mesoscale features of the flow between the Crimean peninsula and southwestern corner of the Turkish coast. The darker areas are the warmer radiated temperatures. Areas that are completely black are clouds. The approximate position of the Rim Current meanders is superimposed on the image.

C1 is expected to be maintained at near-surface levels by the coastal flow derived from river discharges. This coastal current system may be traced on the April 19, 1993, AVHRR image (Fig. 7) by the relatively warmer waters (represented by a darker coastal strip), whereas the cyclonic eddy C1 can be distinguished by a region of shelf waters colder (1.5–2.0°C) than the adjacent region along the continental slope. As described in Section 4, this is more due to the intense convective cooling of the shelf waters during the preceding winter.

Fig. 2 reveals a second meandering, M2, of the Rim Current southwest of the eddy A2 with an indication of another anticyclone, A3, located off Cape Kaliakra of the Bulgarian coast. Unfortunately, the details of the flow field are not captured very well here because of the lack of measurements in the Bulgarian EEZ. But the eddy A3 centered at 43.3°N and 29.8°E is clearly observed in the AVHRR image (Fig. 7). Further south, the Rim Current circulates cyclonically around the southwestern corner of the basin as a tight, intense jet confined to the narrow continental slope region and forms the meander M3. This feature of the Rim Current is also captured very clearly in the satellite image as a band of relatively cold water flowing towards the Bosphorus exit region. Within the narrow shelf zone to its west, an elongated anticyclonic eddy A4 is present.

Sur and Ilyin (1997) presented two additional AVHRR satellite images for 23 and 27 April 1993, which were the only other available cloud free scenes for April or May 1993, and may be used to show evolution of the meandering system within a period of one week. The 27 April image was able to display quite clearly the thermal patterns to the east of 33°E longitude, whereas the features on the other one were restricted to the east of 34°E and along the Turkish coast. All other parts of the basin were covered by clouds. We therefore superimpose this image on the 27 April scene so that we can express all the flow features along the south coast in one composite picture (Fig. 8).

When compared with the previous image of 19 April 1993, Fig. 8 reveals quite clearly evolution and translation of the boundary flow system. In particular, the eddy A1 is stretched meridionally offshore and enlarged to 70 km diameter. The cyclonic meander M1 to the west of it is also intensified. The next anticyclone A2 moved further south to its new center at 43.9°N, 30.6°E. The meanders M2 and M3 are also translated southward by about 50 km. The tip of the meander M3 is now located at 42.2°N and 29.1°E. Three more meanders, which were not noticeable in Fig. 7 due to the cloud coverage, can be seen in this figure downstream of the meander M3 to the east of the Bosphorus.

The Rim current structure inferred from Fig. 8 is reminescent of an energetic unstable boundary flow system, which, as it propogates cyclonically, is modified to the form of large amplitude meanders and filaments. As described previously by Oguz et al. (1994) and shown here in Fig. 9, the September 1991 survey also reveals a highly structured Rim Current pattern in the region. Similar flow configuration along the western coast is also suggested by the May 1994 and April 1995 surveys of R.V. Bilim (figures not shown).

### *3.3. Mesoscale features along the Turkish coast*

The hydrographic data shown in Fig. 2 and the combination of satellite images for 23 and 27 April 1993 (Fig. 8) will aid description of the flow characteristics along the Turkish coast. The six meanders can be identified between the Bosphorus exit and 37°E longitude. Only two of them however, are given by the hydrographic data. Because there were only a few CTD stations along the topographic slope region between TK1 (29.15°E) and TK2 (31.15°E), the flow field shown in Fig. 2 could not capture the large meander M4 (Fig. 8). The half a degree station spacing between the meridional sections to the east of TK2 is too coarse to resolve the flow field properly. In fact, it may be quite misleading since they provide a biased and somewhat different meandering structure of the Rim Current. On the contrary, the satellite images provide correct and more realistic description of the phenomena on the basis of synoptic and much higher resolution data. For example, in the analysis of the hydrographic data, two distinct meanders, M5 and M6, and the accompanying cyclonic eddy between them (Fig. 8) are merged to form one offshore jet along 32°E longitude, with the cyclonic eddy located on its downstream side between the meanders M6 and M7 (Fig. 2). The M6 is one of the most intense meanders of the system and extends approximately 150 km offshore from the coast. The subsequent two meanders (M7 and M8) have more limited offshore extension but cover a relatively

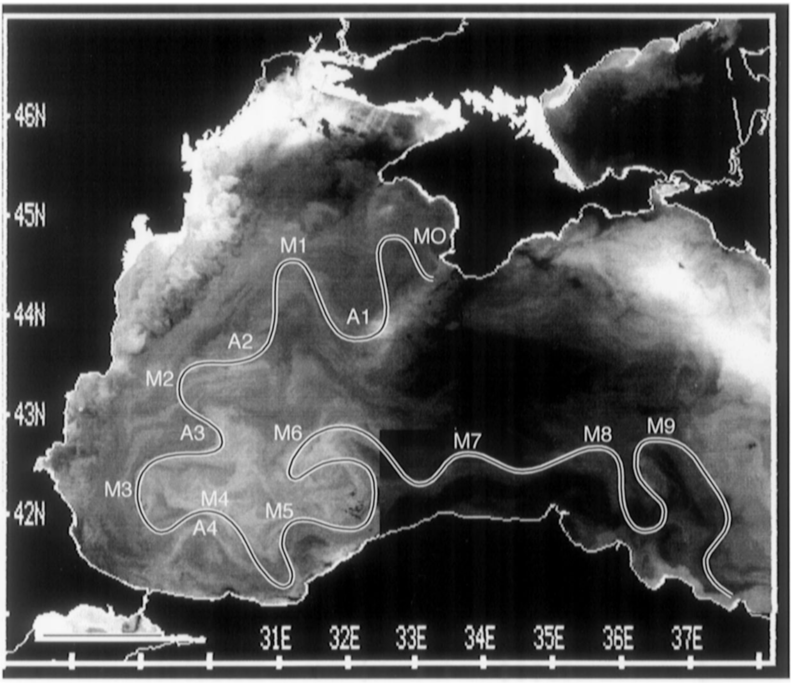


Fig. 8. NOAA 14 AVHRR imagery for 27 April 1993, on which thermal features from 23 April 1993 observed along the Turkish coast between 33°E and 38°E longitude are superimposed for clarity of presentation of the boundary flow structure in the western basin. The darker areas are the warmer radiated temperatures. Areas that are completely black are clouds. The approximate position of the Rim Current meanders is superimposed on the image.

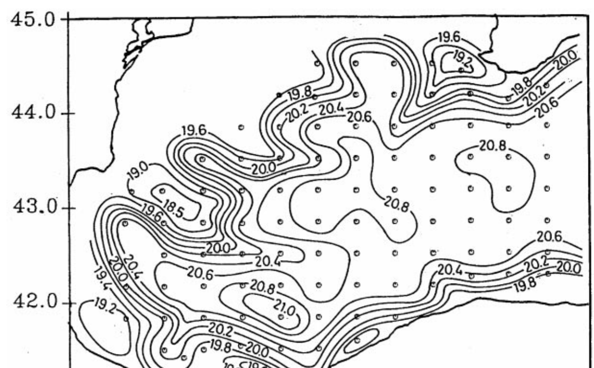


Fig. 9. 100 dbar level salinity distribution during September 1991 (after Oguz et al., 1994), showing meanders of the Rim Current similar to those displayed in Figs. 7 and 8.

wide region between Cape Kerempe (33.5°E) and Cape Sinop (35.5°E). The position of the meander M9 coincides with the Arkhangelsky ridge-trough system, which is known to be one of the major topographic features controlling the boundary flow along the southern coast of the Black Sea (Oguz et al., 1992). The meanders M5, M6, M7, and M8, between 31°E and 36°E longitude, seem to be a quite common configuration. They also emerged in other data sets with different meander amplitude, intensity, phase speed, etc. For example, the meanders during September 1991 (Fig. 9) exhibit a more regular wave pattern, indicating possibly an early stage of meander evolution contrary to the highly developed and energetic features of Fig. 8.

## 4. CIW formation and transport

The NWS and the near-surface levels on top of the thermohaline domes of cyclonic flow in the interior are traditionally known as the sites of dense water formation in winter (Filippov, 1965; Tolmazin, 1985; Ovchinnikov and Popov, 1987). These regions are reported to exhibit vertically homogeneous conditions in response to strong atmospheric cooling, evaporation, and intensified wind mixing associated with a succession of strong, cold and dry continental wind events in the winter season. As the spring warming stratifies the surface water, the convectively generated cold water remains below the seasonal thermocline, and constitutes the so-called Cold Intermediate Layer (CIL) of the upper layer thermohaline structure. Even though this water mass has a considerable importance in the Black Sea ecosystem, our knowledge of its transport characteristics is limited. This issue is revisited here on the basis of new field studies.

As shown in Fig. 10 for section UK1, vertically uniform salinity and temperature structures, with S ~ 18.1–18.2 and T ~ 5°C, are observed throughout the shelf region which provide an indication of CIL formation within the NWS prior to the measure-

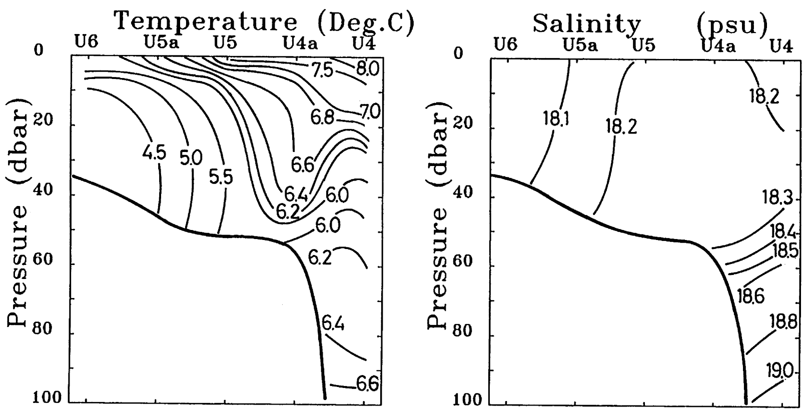


Fig. 10. Temperature (°C) and salinity transects along section UK1.

ments. The survey period corresponds to the initiation of temperature stratification in the surface water as a response to spring warming, which leads to isolation of the cold water patch present within the near-bottom levels of the shelf. The data also provide evidence for the CIW formation event within the cyclonic domes of the western basin's interior. For example, the temperature transect for section TK1 (Fig. 11) reveals a cold water lens with a thickness of 20 m and minimum temperature of 5.5°C on top of the thermocline dome. The vertical uniformity of salinity and density of the water column (S$\sim$18.6, $\sigma_t$ $\sim$14.6 kg/m$^3$) at the same place suggests that the lens is a remnant of the 40 m thick mixed layer formed earlier during the winter. We note that the salinity and density of the mixed layer are higher by about 0.4 and 0.4 kg/m$^3$ as compared with those on the NWS shelf. A similar CIL structure is consistently observed at other meridional sections along the Turkish coast. An example is shown for the cross-section TK5 in Fig. 12. Sections TK1 and TK5 both suggest that the cold water patch slides isopycnally along the periphery of the cyclonic eddies of the interior towards the Rim Current frontal zone, which then transports the cold water cyclonically around the basin.

The transport and spreading characteristics of the shelf CIW seem to be controlled by several processes. A part of this cold water mass is transported by the alongshore

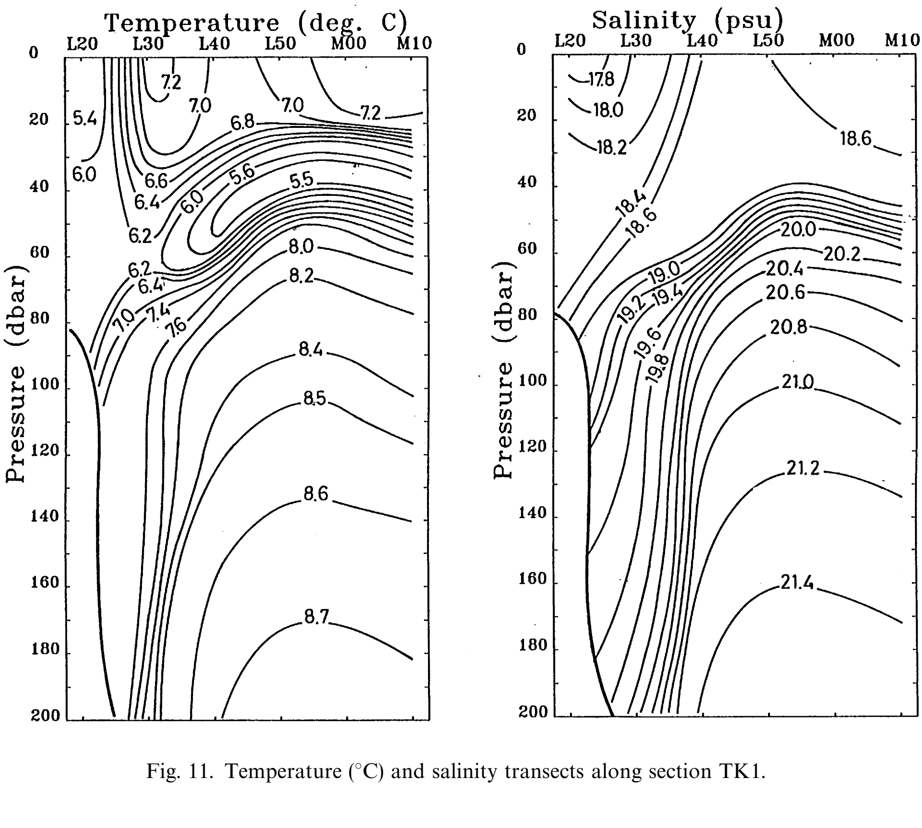


Fig. 11. Temperature (°C) and salinity transects along section TK1.

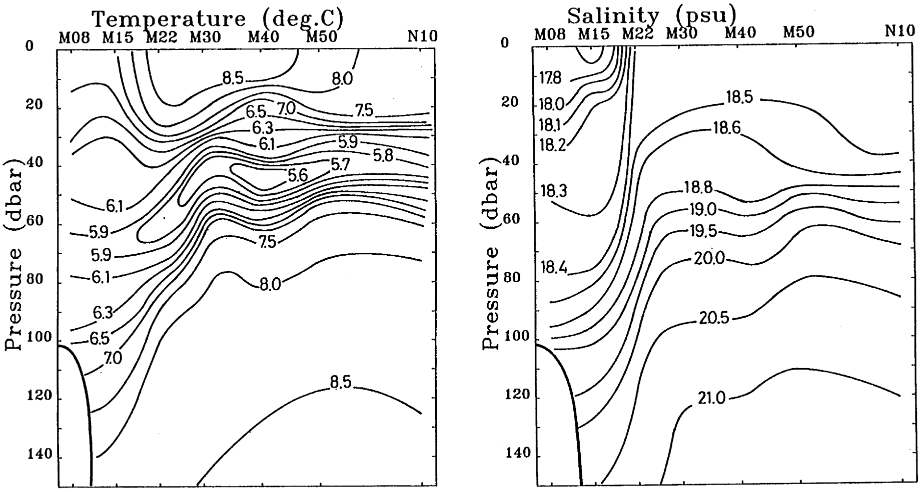


Fig. 12. Temperature (°C) and salinity transects along section TK5.

currents southward on the western shelf. However, because the along shelf currents are relatively weak at this time of the year (typically less than 10 cm/s), which is prior to the beginning of high river run off, this portion of the CIW transport should be relatively small. This may also be inferred from the AVHRR imagery in Fig. 7, where most of the cold water is seen to be trapped within the shelf region. Cold waters carried southward over the shelf might be partially entrained by the coastal mesoscale eddies. Some part of the shelf CIW may be subjected to cross-shelf transport towards the shelf break and slope region, where it flows into the Rim Current convergence zone, similar to the isopycnally sinking cold waters from the deep interior. The Rim Current convergence zone then the location where these two different cold water masses join as they are advected around the periphery of the basin. The April 1993 survey provides excellent examples for such shelf-slope exchanges and their possible modifications due to the mesoscale variability of this zone. These exchange processes, in fact, resemble those taking place along the northeast coast of the United States, as examined in numerous studies such as Houghton et al. (1986), Churchill et al. (1986,1989,1993), Joyce et al. (1992), and Gawarkiewicz et al. (1996).

The temperature transect UK4 (Fig. 13) gives an example of cold water intrusions into the Rim Current convergence zone from the two source regions. The interior cold water mass is transported there (shown in Fig. 13 by stations U18 and U19) by the northwesterly currents of the cyclonic circulation in the interior (see Fig. 2). The cold water mass from the shelf is, on the other hand, supplied by the southeasterly currents along the periphery of the eddy A1, located further west. As a result of continuous supply of the cold water from both sides, the relatively warm water mass confined in the convergence zone is cooled thoroughly. Consequently, a new temperature stratification is developed within the Rim Current zone, in which a cooler and deeper CIL is extended approximately to the 120 m depth.

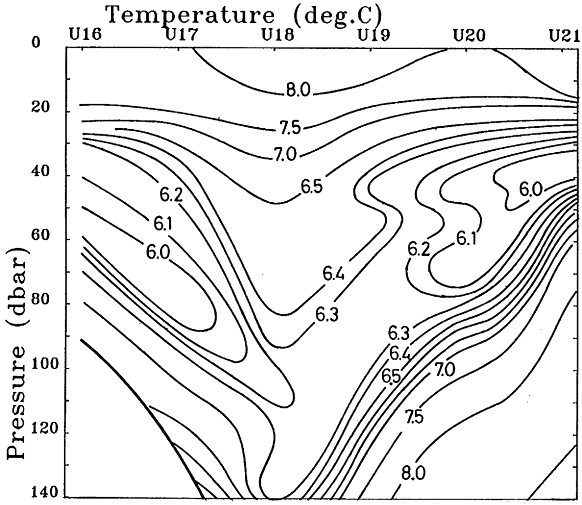


Fig. 13. Temperature (°C) transect along section UK4.

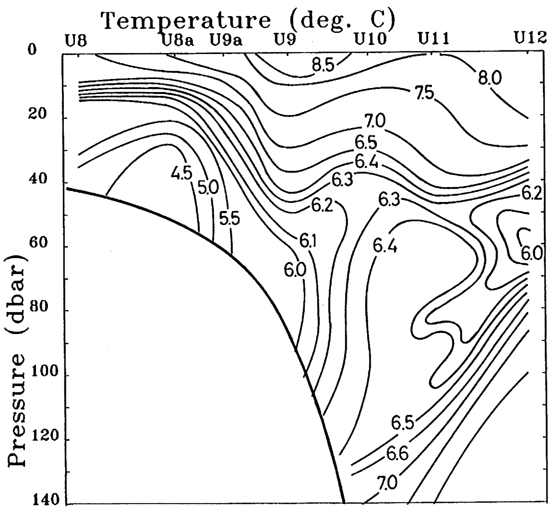


Fig. 14. Temperature (°C) transect along section UK2.

Fig. 14 shows a different type of shelf-slope exchange process along section UK2. As in the previous case, the cold shelf waters are transported towards the shelf break zone by means of the weak southeasterly currents (see Fig. 3). Further intrusion into the Rim Current convergence zone, however, does not take place, since this water mass is blocked near the shelf break by the counter flow of the anticyclonic eddy A1. Consequently, as noted at station U11 in Fig. 14, the relatively warm temperature structure of the eddy is maintained there. The shelf water may, however, be drawn into the convergence zone around the eddy by its peripheral current system. In the presence of such energetic anticyclonic eddies at the shelf break, eddy-induced lateral transport might be a very effective means of bringing the cold shelf water into the convergence zone. Similar speculation is also appropriate for the cyclonic eddies transporting the cold waters from the interior of the basin. Some features of this mechanism were explored along the east coast of United States between the shelf/slope waters and Gulf Stream warm core rings (e.g. Churchill et al., 1986).

## 5. Summary and discussion

Ship mounted ADCP and CTD measurements were carried out in the western Black Sea during 2–15 April 1993. These measurements give insight into several important features of the regional circulation and thermohaline characteristics, which have not been reported before. The principal results are concerned with (i) the strength and three-dimensional structure of the Rim Current flowing cyclonically along the periphery of the basin and the associated mesoscale eddies on its two sides, (ii) documentation of the cold water mass formation event that took place over the shelf and on top of the thermohaline dome of the interior cyclonic circulation in the winter prior to the measurements, (iii) shelf-slope exchanges and transport of the newly formed CIL water by the Rim Current within the basin, and the role of mesoscale structures in these processes.

One of the most striking findings of the April 1993 measurements is the strength of the Rim Current jet. It is typically more than twice that determined from the summer surveys reported in Oguz et al. (1993,1994,1998). Current speeds as high as 1.0 m/s, uniformly distributed within the upper 100 m of the water column, were measured along the jet core with the ADCP in this survey. More interestingly, subpycnocline currents of the order of 20–40 cm/s were recorded between 200 and 350 m, representing the limit of the ADCP measurements. This is the first time (due to availability of the vessel mounted ADCP on R.V. Bilim) that such strong subsurface currents have been reported in the Black Sea. They are almost an order of magnitude stronger than the geostrophically computed currents given in the literature (e.g. Oguz et al., 1993,1994,1998). The latter currents underestimate the vertical jet structure considerably, since they do not include the ageostrophic effects or the barotropic component of the current. Furthermore, the doubled strength of the upper layer geostrophic currents computed from the present data compared with those obtained from the summer surveys of September 1990, 1991 and July 1992 reported elsewhere implies considerable seasonal/interannual variability in the strength of the circulation. Considering the fact that winter 1993 was one of the coldest winters in the region within the last decade, it would be an interesting numerical modeling study to explore the role of such strong cooling on the intensification of the Rim Current system around the periphery of the basin. The other contribution of the ADCP measurements is that it provides more detailed information on the cross-stream structure. Along the Anatolian coast, the shoreward side of the jet is a region of strong anticyclonic shear, typically 30–50 cm/s per 10 km. On the offshore (cyclonic) side, the isotachs are more spread out, but the lateral shear can still attain a value of about 10–20 cm/s per 10 km.

Contrary to the jet-like flow structure over the continental slope, the currents over the northwestern shelf (NWS) are generally less than 10 cm/s. The relative weakness of the shelf currents is, however, consistent with the fact that the continental slope acts as an insulator on the shelf circulation protecting it from the influence of the deep ocean (e.g. Wang, 1982; Chapman and Brink, 1987). The features situated over the so-called "Danube Fan", the wide topographic slope zone between the NWS and the deep interior, have very limited interactions with the shelf circulation. NWS is not much affected by the onshore meanders of the Rim Current, which extends only to the shelf break zone. Accordingly, apart from the contribution of river runoff, the NWS circulation is essentially wind-driven. We however note that, as described earlier by the numerical modeling studies in Oguz et al. (1995) and also reported by various other idealized modeling studies (e.g. Oey and Mellor, 1993; McCreary et al., 1997), the wind and coastal buoyancy forcing tend to generate quite complicated mesoscale circulation over the shelf. An elongated, large cyclonic eddy along the Romanian shelf is first observed in the April 1993 survey and is also seen in the subsequent surveys of May 1994 and April 1995. It remains to be explored, however, how this eddy is modified during the periods of increased fresh water discharges, and when the river plume tends to deflect northward (instead of its usual southward deflection along the coast) as well as in the case of northeasterly winds, both of which promote an anticyclonic circulation within the shelf (Oguz et al., 1995).

The data demonstrate quite clearly that the boundary flow system along the western and soutern coast of the Black Sea possesses meanders and a series of cyclonic–anticyclonic eddy pairs associated with them. They seem to have an amplitude of $\sim$75 km which is larger at two instants ($\sim$125 km for M6 and M9), and longshore wavelengths of 100–125 km. Translation of the features cyclonically around the periphery of the basin, and effects of topographic control as well as instability mechanisms on the flow field are evident in the satellite images. The role of baroclinic instability on the mesoscale structure of the circulation was noted by Blatov et al. (1985) using a simple linear stability analysis of two-layer flows. However, it needs to be studied using more rigorous methods considering the non-linear growth properties of the jet and mean-eddy flow energy transfers.

The present data document the result of the CIW formation event that took place within the NWS and over the dome of the cyclonic gyre of the western basin prior to the measurements. The cold pool on the shelf is found to be relatively colder and fresher than that formed within the near-surface levels of the cyclonic gyre. The shelf CIW has typical salinities of 18.2, whereas the interior CIW is identified by an approximately 0.4 higher salinity. Both of these cold water sources, on the other hand, have similar temperatures of 5–6°C. Thus, the salinity plays a decisive role in distinguishing the origin of the CIW formed in different regions of the sea.

The April 1993 observations suggest the interior basin of the Black Sea as the main source of the CIW formation. The cold water mass formed there eventually sinks towards the periphery of the basin. Recent progress made on the observations and modeling of dense water mass formation and spreading (Marshall and Schott, 1998) points to the crucial role of mesoscale eddies in the process of lateral spreading of dense water masses following its violent convective sinking phase. The role of this mechanism on spreading of CIW during the post-convection phase is not clear and deserves further observational and modeling studies.

Three possible transport mechanisms of the shelf CIW might be identified from the data. The first one is their southward transport by the along-shelf currents. This, however, should comprise only a small percentage since the strength of the along shelf currents are weak in winter and early spring periods, prior to the intensification of river runoff. Furthermore, this water mass should undergo considerable modification as it passes through the coastally attached anticyclonic eddies of the southwestern part of the basin. The second transport mechanism is the off shelf transport to the Rim Current convergence zone, which then advects the CIW around the basin. The data indicate that the anticyclonic eddies located along the shelf break/ upper continental slope topography of the northwestern basin of the Black Sea influence the offshelf transport of the cold water patches. In some cases, they draw cold water filaments seaward and around their peripheries, whereas in other cases they block the offshelf transport and thus cause partial entrapment of the CIW on the shelf. The presence of a cyclonic eddy along the Romanian shelf supports the possibility of long-term residence of the bulk of the CIW on the shelf after its formation, as also noted by the presence of a large cold pool shown in the AVHRR satellite image in Fig. 2b.

## Acknowledgements

This study was accomplished within the framework of the TU-Black Sea Project sponsored by the NATO Science for Stability Program. The field surveys of R.V Bilim and R.V.K. Piri Reis are supported in part by the Turkish Scientific and Technical Research Council. We would like to single out the goverments of Romania and Ukraine for giving permission to work in their waters with the Turkish ship R.V. Bilim. T. Oguz acknowledges the NSF support OCE-9633145, which made possible his visits to MIT in the USA. The manuscript was prepared and put into its final form during these visits. We wish to thank Paola Malanotte-Rizzoli and three anonymous referees. Their constructive remarks improved scientific content of the manuscript.

## References

Blatov, A.S., Ulyanova, V.I., 1985. Effects of curvature of vertical velocity and density profiles on the hydrodynamical instability of a zonal flow. Oceanology (English translation) 25, 11–16.

Chapman, D.C., Brink, K.H., 1987. Shelf and slope circulation induced by fluctuating offshore forcing. Journal of Geophysical Research 92, 11741–11750.

Churchill, J.H., Cornillon, P.C., Milkowski, G.W., 1986. A cyclonic eddy and shelf slope water exchange associated with a Gulf Stream warm-core ring. Journal of Geophysical Research 91 (C8), 9615–9623.

Churchill, J.H., Cornillon, P.C., Hamilton, P., 1989. Velocity and hydrographic structure of subsurface shelf water at the Gulf Stream's edge. Journal of Geophysical Research 94 (C8), 10791–10800.

Churchill, J.H., Levine, E.R., Connors, D.N., Cornillon, P.C., 1993. Mixing of shelf, slope and Gulf Stream water over the continental slope of the Middle Atlantic Bight. Deep-Sea Research I 40, 1063–1085.

Filippov D.M., 1965. The cold intermediate layer in the Black Sea. Oceanology (English translation) 5, 47-52.

Firing, E., 1991. Acoustic Doppler current profiling measurements and navigation. WOCE Hydrographic Program Office Rep. WHPO 91-9, WOCE Rep. 68/91, 24 pp.

Gawarkiewicz, G., Ferdelman, T.G., Church, T.M., Luther III, G.W., 1996. Shelfbreak frontal structure on the continental shelf north of Cape Hatteras. Continental Shelf Research 16 (14), 1751–1773.

Gungor, H., 1994. Multivariate objective analyses of ADCP and CTD measurements applied to the circulation of the Levantine Sea and the Black Sea. M.Sc. Thesis, Institute of Marine Sciences, Middle East Technical University, 78pp.

Houghton, R.W., Olson, D.B., Celone, P.J., 1986. Observation of an anticyclonic eddy near the continental shelf break south of New England. Journal of Physical Oceanography 16, 60–71.

Joyce, T.M., Bishop, J.K.B., Brown, O.B. 1992. Observations of offshore shelf-water transport induced by a warm-core ring. Deep-Sea Research, 39 (Supplement), I, S97-S113.

McCreary Jr., J.P., Zhang, S., Shetye, S., 1997. Coastal circulations driven by river outflow in a variable density 1.5 layer model. Journal of Geophysical Research 102, 15535–15554.

Marshall, J., Schott, F., 1998. Open ocean convection: Observations, theory and models. Massachusetts Institute of Technology, Center for Global Change Science, Report No.52, 158 pp.

McWilliams, J.C., Owens, W.B., Hua, B.L., 1986. An objective analysis of the POLYMODE Local Dynamical Experiment. Part I: general formalism and statistical analysis. Journal of Physical Oceanography 16, 483–504.

Oey, L.Y., Mellor, G., 1993. Subtidal variability of estuarine outflow, plume and coastal current: a model study. Journal of Physical Oceanography 23, 164–171.

Oguz, T., La Violette, P.E., Unluata, U., 1992. The upper layer circulation of the Black Sea: its variability as inferred from hydrographic and satellite observations. Journal of Geophysical Research 97, 12569–12584.

Oguz, T., Latun, V.S., Latif, M.A., Vladimirov, V.V., Sur, H.I., Markov, A.A., Ozsoy, E., Kotovshchikov, B.B., Eremeev, V.V., Unluata, U., 1993. Circulation in the surface and intermediate layers of the Black Sea. Deep-Sea Research I 40, 1597–1612.

Oguz, T., Aubrey, D.G., Latun, V.S., Demirov, E., Koveshnikov, L., Diaconu, V., Sur, H.I., Besiktepe, S., Duman, M., Limeburner, R., Eremeev, V., 1994. Mesoscale circulation and thermohaline structure of the Black Sea observed during Hydro Black'91. Deep-Sea Research I 41, 603–628.

Oguz, T., Malanotte-Rizzoli, P., Aubrey, D.G., 1995. Wind and thermohaline circulation of the Black Sea driven by yearly mean climatological forcing. Journal of Geophysical Research 100, 6845–6863.

Oguz, T., Ivanov, L.I., Besiktepe, S., 1998. Circulation and Hydrographic characteristics of the Black Sea during 1992. In: Ivanov, L.I., Oguz, T. (Eds.), Ecosystem Modeling as a Management Tool for the Black Sea, Vol. 2, NATO ASI Series 2. Environmental Security, Vol. 47 Kluwer Academic Publishers, Dordrecht, pp. 69–92.

Ovchinnikov, I.M., Popov, Yu. I., 1987. Evolution of the cold intermediate layer in the Black Sea. Oceanology (English translation) 27, 555–560.

Ovchinnikov, I.M., Titov, V.B., Krivosheya, V.G., Popov, Yu. I., 1994. Major fluid dynamical processes and their role in the ecology of waters of the Black Sea. Oceanology (English translation) 33, 707–712.

Sur, H.I., Ozsoy, E., Unluata, U., 1994. Boundary current instabilities, upwelling, shelf mixing and eutrophication processes in the Black Sea. Progress in Oceanography 33, 249–302.

Sur, H.I., Ozsoy, E., Ilyin, Y.P., Unluata, U., 1996. Coastal-deep ocean interactions in the Black Sea and their ecological/environmental impacts. Journal of Marine Systems 7, 293–320.

Sur, H.I., Ilyin, Y.P., 1997. Evolution of satellite derived mesoscale thermal patterns in the Black Sea. Progress in Oceanography 39, 109–151.

Tolmazin, D., 1985. Changing coastal oceanography of the Black Sea — I: North- western shelf. Progress in Oceanography 15, 217–276.

Wang, D.P., 1982. Effects of continental slope on the mean shelf circulation. Journal of Physical Oceanography 12, 1524–1526.